Supplemental Material for "Synthetic spin-orbit coupling in an optical lattice clock"

Interaction Hamiltonian with the spin model assumption The Hamiltonian governing fermionic AEAs in an optical lattice clock may be written:

$$\hat{H} = \hat{H}_0 + \hat{H}_I + \hat{H}_L \,, \tag{S1}$$

$$\hat{H}_0 = \sum_{\alpha} \int d\mathbf{r} \hat{\psi}_{\alpha}(\mathbf{r}) \left[-\frac{\hbar^2}{2m}\nabla^2 + V_{\text{ext}}(\mathbf{r}) \right] \hat{\psi}_{\alpha}(\mathbf{r}) - \hbar\delta \int d\mathbf{r} \hat{\psi}_e^{\dagger}(\mathbf{r}) \hat{\psi}_e(\mathbf{r}) \,, \tag{S2}$$

$$\hat{H}_I = \frac{4\pi\hbar^2 a_{eg}^-}{m} \int d\mathbf{r} \hat{\psi}_e^{\dagger}(\mathbf{r}) \hat{\psi}_e(\mathbf{r}) \hat{\psi}_g^{\dagger}(\mathbf{r}) \hat{\psi}_g(\mathbf{r}) + \sum_{\alpha\beta} \frac{3\pi\hbar^2 b_{\alpha\beta}^3}{m} \int d\mathbf{r} W\left[\hat{\psi}_{\alpha}^{\dagger}(\mathbf{r}), \hat{\psi}_{\beta}^{\dagger}(\mathbf{r})\right] \left(W\left[\hat{\psi}_{\alpha}^{\dagger}(\mathbf{r}), \hat{\psi}_{\beta}^{\dagger}(\mathbf{r})\right]\right)^{\dagger} \,, \tag{S3}$$

$$\hat{H}_L = -\frac{\hbar\Omega}{2} \int d\mathbf{r} \left[\hat{\psi}_e^{\dagger}(\mathbf{r}) e^{i2\pi Z/\lambda} \hat{\psi}_g(\mathbf{r}) + \text{H.c.} \right] \tag{S4}$$

where m is the atomic mass, $\hat{\psi}_{\alpha}(\mathbf{r})$ is a fermionic field operator for state $\alpha \in \{g, e\}$, $W\left[\hat{A}(\mathbf{r}), \hat{B}(\mathbf{r})\right] = (\nabla \hat{A}(\mathbf{r}))\hat{B}(\mathbf{r}) - \hat{A}(\mathbf{r})(\nabla \hat{B}(\mathbf{r}))$ is the Wronskian, and $\delta = \omega_l - \omega_0$ is the difference between the clock laser frequency ω_l and atomic frequency ω_0 in the rotating frame of the laser. The Hamiltonian $\hat{H}_0$ contains the kinetic energy and trapping potential $V_{\text{ext}}(\mathbf{r})$, $\hat{H}_I$ contains the effects of s-wave interactions with scattering length a_{eg}^- and p-wave interactions with interaction volumes $b_{\alpha\beta}^3$ between nuclear spin-polarized AEAs, and $\hat{H}_L$ describes the coupling of internal levels to the clock laser. We assume that the optical lattice is deep enough that we can neglect interactions occurring between different lattice sites, and so consider only interactions between particles occupying the same lattice site. Further, we enact the spin model approximation [1], which neglects all interactions which do not preserve the single-particle transverse mode occupations during a two-body collision. The spin model Hamiltonian hence keeps only direct terms, in which the two colliding particles remain in their same transverse motional quantum states, and exchange processes where the transverse quantum numbers of the two colliding particles are exchanged. The spin model Hamiltonian is valid when interactions are smaller than the spacing between transverse modes, and also when anharmonicity of the potential prevents collisional exchange of mode energy between transverse dimensions.

To derive a Hubbard model amenable for direct calculation, we expand the field operators in a basis of single-particle eigenfunctions. In order to facilitate thermal averages, we take this set of functions to be the eigenfunctions of $\hat{H}_0$, $\psi_{q,n}(\mathbf{r})$, which are indexed in terms of a quasimomentum q and a transverse mode index $\mathbf{n}$. Enacting this expansion with the approximations of the last paragraph, we find

$$\begin{aligned}\hat{H}_I = \frac{1}{4L} \sum_{\alpha\beta} \sum_{\{\mathbf{n}_1,\mathbf{n}_2\}} \sum_{qq'\Delta q} \Big[&(2-\delta_{\mathbf{n}_1\mathbf{n}_2}) \left(U^{\alpha\beta}_{\{\mathbf{n}_1,\mathbf{n}_2\}} + V^{\alpha\beta}_{\{\mathbf{n}_1,\mathbf{n}_2\}} \right) \hat{a}^{\dagger}_{\alpha,q+\Delta q,\mathbf{n}_1} \hat{a}^{\dagger}_{\beta,q'-\Delta q,\mathbf{n}_2} \hat{a}_{\beta,q',\mathbf{n}_2} \hat{a}_{\alpha,q,\mathbf{n}_1} \\ &+ 2(1-\delta_{\mathbf{n}_1\mathbf{n}_2}) \left(V^{\alpha\beta}_{\{\mathbf{n}_1,\mathbf{n}_2\}} - U^{\alpha\beta}_{\{\mathbf{n}_1,\mathbf{n}_2\}} \right) \hat{a}^{\dagger}_{\beta,q'-\Delta q,\mathbf{n}_1} \hat{a}^{\dagger}_{\alpha,q+\Delta q,\mathbf{n}_2} \hat{a}_{\beta,q',\mathbf{n}_2} \hat{a}_{\alpha,q,\mathbf{n}_1} \Big] \,.\end{aligned} \tag{S5}$$

Here, L is the number of lattice sites, the sum over $\{\mathbf{n}_1, \mathbf{n}_2\}$ means the sum over distinct, ordered pairs of transverse modes, q, q', and Δq are quasimomenta in the first Brillouin zone (BZ), greek letters denote internal electronic states $\alpha, \beta \in \{g, e\}$, and the interaction matrix elements may be written as

$$U^{\alpha\beta}_{\{\mathbf{n}_1,\mathbf{n}_2\}} = (1-\delta_{\alpha\beta}) \frac{8\pi\hbar^2}{m} a_s S_{\mathbf{n}_1\mathbf{n}_2\mathbf{n}_2\mathbf{n}_1} \,, \quad V^{\alpha\beta}_{\{\mathbf{n}_1,\mathbf{n}_2\}} = \frac{12\pi\hbar^2}{m} b^3_{\alpha\beta} P_{\mathbf{n}_1\mathbf{n}_2\mathbf{n}_2\mathbf{n}_1} \tag{S6}$$

by defining the integrals

$$S_{\mathbf{n}_1'\mathbf{n}_2'\mathbf{n}_2\mathbf{n}_1} = \int d\mathbf{r} \psi^{\star}_{i,\mathbf{n}_1'}(\mathbf{r}) \psi^{\star}_{i,\mathbf{n}_2'}(\mathbf{r}) \psi_{i,\mathbf{n}_2}(\mathbf{r}) \psi_{i,\mathbf{n}_1}(\mathbf{r}) \,, \quad P_{\mathbf{n}_1'\mathbf{n}_2'\mathbf{n}_2\mathbf{n}_1} = \int d\mathbf{r} W\left[\psi^{\star}_{i,\mathbf{n}_1'}(\mathbf{r}), \psi^{\star}_{i,\mathbf{n}_2'}(\mathbf{r})\right] W\left[\psi_{i,\mathbf{n}_1}(\mathbf{r}), \psi_{i,\mathbf{n}_2}(\mathbf{r})\right] \,. \tag{S7}$$

In the latter two expressions, the wavefunctions are localized Wannier-type functions obtained from the quasimomentum-indexed eigensolutions (Bloch functions) of the full 3D potential as $\psi_{j,\mathbf{n}}(\mathbf{r}) =$

$\frac{1}{\sqrt{L}}\sum_{q\in \mathrm{BZ}} e^{-iqr_j}\psi_{q,\mathbf{n}}(\mathbf{r})$ [2]. We can also define the mode-dependent tunneling and Rabi frequency in terms of these functions as

$$J_{\mathbf{n}} = -\int d\mathbf{r}\psi_{j,\mathbf{n}}(\mathbf{r})\left[-\frac{\hbar^2}{2m}\nabla^2 + V_{\mathrm{ext}}(\mathbf{r})\right]\psi_{j+1,\mathbf{n}}(\mathbf{r})\ , \tag{S8}$$

$$\Omega_{\mathbf{n}} = \Omega\int d\mathbf{r}\psi_{j,\mathbf{n}}(\mathbf{r})\, e^{i2\pi Z/\lambda}\psi_{j,\mathbf{n}}(\mathbf{r})\ . \tag{S9}$$

First-order density shift in Ramsey spectroscopy In this section we compute the density shift for Ramsey spectroscopy to first order in interactions using an interaction picture perturbation series. In particular, we write the propagator during the dark time evolution in terms of a truncated Dyson series $e^{-i\hat{H}t} = e^{-i\hat{H}_0 t} - i\int_0^t dt' e^{-i\hat{H}_0(t-t')}\hat{H}_1 e^{-i\hat{H}_0 t'}$. At the end of the dark time, a spin-rotation pulse of area θ_2 is applied, and then the total $\hat{S}^z$ is measured. These two operations can be combined as the measurement of the operator $\hat{S}^z_\theta = \sum_{nq}\left[\cos\theta \hat{S}^z_{q\mathbf{n}} - \sin\theta\hat{S}^y_{q\mathbf{n}}\right]$. Hence, the first-order result of the Ramsey sequence is

$$\langle \hat{S}^z(\tau)\rangle = \langle\psi(\theta_1)|e^{i\hat{H}_0\tau}\hat{S}^z_{\theta_2}e^{-i\hat{H}_0\tau}|\psi(\theta_1)\rangle + 2\mathcal{I}\left[\langle\psi(\theta_1)|e^{i\hat{H}_0\tau}\hat{S}^z_{\theta_2}\int_0^\tau dt e^{-i\hat{H}_0(\tau-t)}\hat{H}_I e^{-i\hat{H}_0 t}|\psi(\theta_1)\rangle\right]\ , \tag{S10}$$

where $|\psi(\theta_1)\rangle$ is the state resulting from applying the first Ramsey pulse to an initial state $|\tilde{i}\rangle$. We will parameterize the initial state in terms of products of single-particle eigenstates $|i\rangle = \prod_{i=1}^N \hat{a}^\dagger_{gq_in_i}|\mathrm{vac.}\rangle$, where $|\mathrm{vac.}\rangle$ is the vacuum, N the number of particles, and $\{q_i, \mathbf{n}_i\}$ the initial distinct set of populated quasimomenta and transverse modes, so that

$$|\psi(\theta_1)\rangle = \prod_{j=1}^N\left(\cos\frac{\theta_1}{2}\hat{a}^\dagger_{g,q_j,\mathbf{n}_j} + i\sin\frac{\theta_1}{2}\hat{a}^\dagger_{e,q_j,\mathbf{n}_j}\right)\ . \tag{S11}$$

From this, we find that the non-interacting dynamics are given as

$$\langle\psi(\theta_1)|e^{i\hat{H}_0\tau}\hat{S}^z_{\theta_2}e^{-i\hat{H}_0\tau}|\psi(\theta_1)\rangle = \sum_{i=1}^N\left[-\frac{\cos\theta_1\cos\theta_2}{2} + \frac{\sin\theta_1\sin\theta_2}{2}\cos\left(\delta\tau - \Delta E_{\mathbf{n}_i}(q_i,\phi)\tau\right)\right]\ , \tag{S12}$$

where $E_{\mathbf{n}}(q)$ is the single-particle dispersion and

$$\Delta E_{\mathbf{n}}(q,\phi) \equiv E_{\mathbf{n}}(q+\phi) - E_{\mathbf{n}}(q)\ , \tag{S13}$$

is the difference in single-particle dispersion of the e and g states.

Writing the non-interacting result as $\langle\hat{S}^z(\tau)\rangle = A(\tau)\cos(\delta\tau) + B(\tau)\sin(\delta\tau) + \mathrm{const.}$ we can extract the density shift as $\Delta\nu = \frac{1}{2\pi\tau}\arctan\left(\frac{B(\tau)}{A(\tau)}\right)$ and the normalized contrast decay as $\mathcal{C}(\tau) = \frac{\sqrt{A^2(\tau)+B^2(\tau)}}{\sqrt{A^2(0)+B^2(0)}}$. For a single particle with momentum q and transverse mode n, the density shift is $\Delta E_{\mathbf{n}}(q,\phi)/2\pi$. Assuming short times compared to the tunneling bandwidth, the density shifts for all particles add as $\Delta\nu = \sum_{i=1}^N \Delta E_{\mathbf{n}_i}(q_i,\phi)/2\pi N + \mathcal{O}(\tau^2)$. The contrast decay at short times is given as $\mathcal{C}(\tau) = 1 - \frac{1}{2N^2}\left(\sum_{i=1}^N\Delta E_{\mathbf{n}_i}(q_i,\phi)\right)^2\tau^2 + \frac{1}{2N}\sum_{i=1}^N\Delta E^2_{\mathbf{n}_i}(q_i,\phi)\tau^2 + \mathcal{O}(\tau^4)$. This single-particle contribution will dominate over the $\sim U^2\tau^2$ decay of the contrast due to interactions at short times and in the regime of weak interactions compared to the tunneling.

The contribution to the dynamics at the lowest order in interactions is given as

$$\begin{aligned}
&2\mathcal{I}\left[\langle\psi(\theta_1)|e^{i\hat{H}_0\tau}\hat{S}^z_{\theta_2}\int_0^\tau dt e^{-i\hat{H}_0(\tau-t)}\hat{H}_I e^{-i\hat{H}_0 t}|\psi(\theta_1)\rangle\right] \qquad\qquad (\mathrm{S14})\\
&= \frac{\tau}{L}\sum_{\{p_1,p_2\}}\Bigg\{\sin\theta_1\sin\theta_2\sin\left[\left(\delta - \frac{\Delta E_{\mathbf{n}_{p_1}}(q_{p_1},\phi) + \Delta E_{\mathbf{n}_{p_2}}(q_{p_2},\phi)}{2}\right)\tau\right]\\
&\times\Bigg[\left(C_{\{\mathbf{n}_{p_1}\mathbf{n}_{p_2}\}} - \chi_{\{\mathbf{n}_{p_1}\mathbf{n}_{p_2}\}}\cos\theta_1\right)\cos\left(\frac{\Delta E_{\mathbf{n}_{p_1}}(q_{p_1},\phi) - \Delta E_{\mathbf{n}_{p_2}}(q_{p_2},\phi)}{2}\tau\right)\\
&-\frac{\cos\theta_1}{2}\left(2-\delta_{\mathbf{n}_{p_1}\mathbf{n}_{p_2}}\right)\zeta_{\{\mathbf{n}_{p_1}\mathbf{n}_{p_2}\}}\left[\cos\left(\frac{\Delta E_{\mathbf{n}_{p_1}}(q_{p_1},\phi) - \Delta E_{\mathbf{n}_{p_2}}(q_{p_2},\phi)}{2}\tau\right) - \mathrm{sinc}\left(\frac{\Delta E_{\mathbf{n}_{p_1}}(q_{p_1},\phi) - \Delta E_{\mathbf{n}_{p_2}}(q_{p_2},\phi)}{2}\tau\right)\right]\Bigg]\Bigg\}
\end{aligned}$$

where the mode-dependent spin model parameters are

$$C_{\{\mathbf{n}_1\mathbf{n}_2\}} = \frac{V^{ee}_{\{\mathbf{n}_1\mathbf{n}_2\}} - V^{gg}_{\{\mathbf{n}_1\mathbf{n}_2\}}}{2} \tag{S15}$$

$$\chi_{\{\mathbf{n}_1\mathbf{n}_2\}} = \frac{V^{ee}_{\{\mathbf{n}_1\mathbf{n}_2\}} + V^{gg}_{\{\mathbf{n}_1\mathbf{n}_2\}} - 2V^{ge}_{\{\mathbf{n}_1\mathbf{n}_2\}}}{2} \tag{S16}$$

$$\zeta_{\{\mathbf{n}_1\mathbf{n}_2\}} = \frac{V^{eg}_{\{\mathbf{n}_1\mathbf{n}_2\}} - U^{ge}_{\{\mathbf{n}_1\mathbf{n}_2\}}}{2} \,. \tag{S17}$$

Taking a series in the tunneling bandwidth, the zeroth order term for a given pair of particles is $(C - \chi\cos\theta_1)\sin\theta_1\sin\theta_2\sin\delta\tau$, which has been obtained in previous works [3]. The thermally averaged density shift in the high-temperature limit will be given in the next section.

High-temperature thermal average of density shift Here, we derive the high-temperature (compared to the tunneling bandwidth) thermal average of the first-order many-body dynamics derived in the last section. First, we expand the above result to third order in time, finding

$$\begin{aligned}
\langle \hat{S}^z(\tau)\rangle = {} & \frac{1}{2}\sum_{i=1}^{N}\left(\cos(\delta\tau)\sin\theta_1\sin\theta_2 - \cos\theta_1\cos\theta_2\right) \\
& + \sum_{\{p_1,p_2\}}\frac{\sin\theta_1\sin\theta_2}{L}\tau\left(C_{\{\mathbf{n}_{p_1},\mathbf{n}_{p_2}\}} - \chi_{\{\mathbf{n}_{p_1},\mathbf{n}_{p_2}\}}\cos\theta_1\right)\sin\delta\tau + \frac{1}{2}\sum_{i=1}^{N}\Delta E_{\mathbf{n}_i}(q_i,\phi)\sin(\delta\tau)\sin\theta_1\sin\theta_2\tau \\
& - \sum_{\{p_1,p_2\}}\frac{\sin\theta_1\sin\theta_2}{L}\frac{\tau^2}{2}\left(C_{\{\mathbf{n}_{p_1},\mathbf{n}_{p_2}\}} - \chi_{\{\mathbf{n}_{p_1},\mathbf{n}_{p_2}\}}\cos\theta_1\right)\left(\Delta E_{\mathbf{n}_{p_1}}(q_{p_1},\phi) + \Delta E_{\mathbf{n}_{p_2}}(q_{p_2},\phi)\right)\cos\delta\tau \\
& - \frac{1}{4}\sum_{i=1}^{N}\Delta E_{\mathbf{n}_i}(q_i,\phi)^2\cos(\delta\tau)\sin\theta_1\sin\theta_2\tau^2 \\
& - \sum_{\{p_1,p_2\}}\frac{\sin\theta_1\sin\theta_2}{L}\frac{\tau^3}{24}\Big[6\left(C_{\{\mathbf{n}_{p_1},\mathbf{n}_{p_2}\}} - \chi_{\{\mathbf{n}_{p_1},\mathbf{n}_{p_2}\}}\cos\theta_1\right)\left(\Delta E_{\mathbf{n}_{p_1}}(q_{p_1},\phi)^2 + \Delta E_{\mathbf{n}_{p_2}}(q_{p_2},\phi)^2\right) \\
& - \left(2 - \delta_{\mathbf{n}_{p_1}\mathbf{n}_{p_2}}\right)\zeta_{\{\mathbf{n}_{p_1},\mathbf{n}_{p_2}\}}\left(\Delta E_{\mathbf{n}_{p_1}}(q_{p_1},\phi) - \Delta E_{\mathbf{n}_{p_2}}(q_{p_2},\phi)\right)^2\cos\theta_1\sin\delta\tau\Big] \\
& - \frac{1}{12}\sum_{i=1}^{N}\Delta E_{\mathbf{n}_i}(q_i,\phi)^3\sin(\delta\tau)\sin\theta_1\sin\theta_2\tau^3\Big\} \,.
\end{aligned} \tag{S18}$$

To perform thermal averages, we now enact the tight-binding approximation, in which $E_{\mathbf{n}}(q) = \bar{E}_{\mathbf{n}} - 2J_{\mathbf{n}}\cos(q)$, and compute the partition function as

$$Z = \sum_{nq} e^{-\beta E_{\mathbf{n}}(q)} \approx \sum_{\mathbf{n}} e^{-\beta\bar{E}_{\mathbf{n}}}\int_{-1}^{1} dq e^{2\beta J_{\mathbf{n}}\cos(\pi q)} \tag{S19}$$

$$= 2\sum_{\mathbf{n}} e^{-\beta\bar{E}_{\mathbf{n}}} I_0(2\beta J_{\mathbf{n}}) = 2\sum_{\mathbf{n}} e^{-\beta\bar{E}_{\mathbf{n}}}\left[1 + \mathcal{O}\left(\beta^2 J_{\mathbf{n}}^2\right)\right] \,, \tag{S20}$$

where $I_\nu(x)$ is the modified Bessel function of order ν and β the inverse radial temperature. Hence, for temperatures sufficiently high compared to the bandwidth $J_{\mathbf{n}}$, the partition function is just a constant times the partition function of the transverse modes. Now,

$$\langle \Delta E_n(q,\phi)\rangle_{T_R} = \frac{1}{Z}\sum_{\mathbf{n}} e^{-\beta\bar{E}_{\mathbf{n}}} 4J_{\mathbf{n}}(1 - \cos\phi)\, I_1(2\beta J_{\mathbf{n}}) \tag{S21}$$

$$= \frac{1}{Z_{\mathbf{n}}}\sum_{\mathbf{n}} e^{-\beta\bar{E}_{\mathbf{n}}} 2\beta J_{\mathbf{n}}(1 - \cos\phi) + \mathcal{O}\left(\beta^2 J_{\mathbf{n}}^2\right) \,, \tag{S22}$$

where $Z_{\mathbf{n}} = \sum_{\mathbf{n}} e^{-\beta\bar{E}_{\mathbf{n}}}$ is the partition function of the transverse modes. This result gives that terms which are linear in $\Delta E_{\mathbf{n}}(q,\phi)$ for a specific q, including terms like $\Delta E_{\mathbf{n}_1}(q_1,\phi)\,\Delta E_{\mathbf{n}_2}(q_2,\phi)$, vanish at least as fast as $\mathcal{O}(\beta)$ at high temperatures. In contrast, we find

$$\langle \Delta E_{\mathbf{n}}^2 (q,\phi)\rangle_{T_R} = \frac{1}{Z}\sum_{\mathbf{n}} e^{-\beta \bar{E}_{\mathbf{n}}} 16 J_{\mathbf{n}}^2 \Big[\frac{1}{\beta J_{\mathbf{n}}} I_1(2\beta J_{\mathbf{n}}) + I_2(2\beta J_{\mathbf{n}})(1-\cos\phi)\Big]\sin^2\frac{\phi}{2}$$
$$= \frac{1}{Z_{\mathbf{n}}}\sum_{\mathbf{n}} e^{-\beta \bar{E}_{\mathbf{n}}} 4 J_{\mathbf{n}}^2 (1-\cos\phi) + \mathcal{O}\left(\beta^2 J_{\mathbf{n}}^2\right)\,, \tag{S23}$$

and so the thermal average of $\Delta E_{\mathbf{n}}^2(q,\phi)$ is a constant to lowest order in a high-temperature expansion.

Using these results, we find that the leading order approximation in a high-temperature series expansion is

$$\langle\langle \hat{S}_{\theta_2}^z\rangle\rangle_{T_R} = \frac{N}{2}\left(\sin\theta_1\sin\theta_2\cos(\delta\tau) - \cos\theta_1\cos\theta_2\right) + \frac{\tau N(N-1)}{2L}\sin\theta_1\sin\theta_2\sin(\delta\tau)\left(\langle C\rangle_{T_R} - \langle\chi\rangle_{T_R}\cos\theta_1\right)$$
$$-2N\langle J^2\rangle_{T_R}\sin\theta_1\sin\theta_2\cos(\delta\tau)\sin^2\frac{\phi}{2}\tau^2 - \frac{\langle J^2\rangle_{T_R}\tau^3 N(N-1)}{6}\sin^2\frac{\phi}{2}\left[6\left(\langle C\rangle_{T_R} - \langle\chi\rangle_{T_R}\cos\theta_1\right) - 2\langle\zeta\rangle_{T_R}\cos\theta_1\right]\,, \tag{S24}$$

where we have neglected interactions between pairs of particles with the same transverse mode for simplicity, $\langle\bullet\rangle_{T_R}$ denotes a thermal average with respect to the transverse modes, and we have assumed that, e.g. $\langle J^2 C\rangle_{T_R} \approx \langle J^2\rangle_{T_R}\langle C\rangle_{T_R}$, which is valid when the tunneling is only weakly temperature dependent. From this, we find the density shift

$$\Delta\nu = \Delta\nu_0\left[1 + \frac{4}{3}\langle J^2\rangle_{T_R}\tau^2\sin^2\frac{\phi}{2}\frac{\langle\zeta\rangle_{T_R}\cos\theta_1}{\langle C\rangle_{T_R} - \langle\chi\rangle_{T_R}\cos\theta_1}\right]\,, \tag{S25}$$

where $\Delta\nu_0$ is the density shift in the absence of tunneling.

Lineshape and extraction of $\theta_{\mathbf{n}q}$ from momentum-resolved Rabi spectroscopy

As described in the main text, SOC introduces substructure in the Rabi lineshape within a window of width $8J_{\mathbf{n}}\left|\sin\frac{\phi}{2}\right|$ of the carrier frequency. At finite temperature, many transverse modes are populated and hence the dependence of $\Omega_{\mathbf{n}}$ and $J_{\mathbf{n}}$ on $\mathbf{n}$ could broaden the line and destroy this substructure. However, a direct simulation of the Rabi lineshape using the potential Eq. (1) demonstrates that the features of the ideal, zero-temperature lineshape are captured up to a temperature of 3μK as shown in Fig. 1(a). Thanks to the clock's sub-Hz resolution it will be possible to resolve the lineshape for a wide range of lattice parameters.

We now turn to the extraction of the chiral Bloch vector angle $\theta_{\mathbf{n}q}$ with Rabi spectroscopy. The eigenstates of Eq. (3) may be written as

$$|\psi_{n,q,-}\rangle = \cos\frac{\theta_{nq}}{2}|gqn\rangle + \sin\frac{\theta_{nq}}{2}|eqn\rangle \tag{S26}$$
$$|\psi_{n,q,+}\rangle = -\sin\frac{\theta_{nq}}{2}|gqn\rangle + \cos\frac{\theta_{nq}}{2}|eqn\rangle\,, \tag{S27}$$

with energies

$$E_{n,q,\pm} = \frac{E_n(q) + E_n(q+\phi) + \delta}{2} \pm |\mathbf{B}_{nq}|\,, \tag{S28}$$

and magnetization

$$\langle\psi_{n,q,\pm}|\hat{S}_{n,q}^z|\psi_{n,q,\pm}\rangle = \frac{\pm\cos\theta_{nq}}{2}\,. \tag{S29}$$

Using the above, the expected Rabi dynamics in the ideal case for an arbitrary initial state $\alpha|g\mathbf{n}q\rangle + \beta|e\mathbf{n}q\rangle$ is found to be

$$S^z(\alpha,\beta,t) = \frac{1}{2}\left(|\beta|^2 - |\alpha|^2\right)\left[\cos^2\theta_{nq} + \cos(2B_{nq}t)\sin^2\theta_{nq}\right] + \mathcal{R}(\alpha^\star\beta)\cos\theta_{nq}\sin\theta_{nq}\left(\cos(2B_{nq}t) - 1\right)$$
$$+\mathcal{I}(\alpha^\star\beta)\sin\theta_{nq}\sin(2B_{nq}t)\,. \tag{S30}$$

The protocol extracting the chiral Bloch vector angle $\theta_{\mathbf{n}q}$ involves three sequences (Fig. 1(b)). All sequences start by preparing the atoms in g. In sequence I, a narrow π-pulse about the x axis is applied at the detuning $\delta^\star$ associated with the $q_{\mathbf{0}}^\star$ resonance. The Rabi frequency of the pulse, $\Omega_{\mathbf{0}}^p$, should be weak enough to guarantee that only atoms

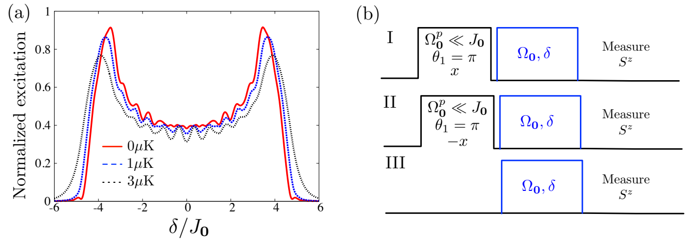

FIG. 1. (Color online) (a) Thermally averaged Rabi lineshape fully accounting for trap non-separability. SOC-induced peaks are visible even at $T = 3\mu$K. (b) Three pulse sequences used to extract $\theta_{\mathbf{0}q}$ in Fig. (2) of the main text.

within a narrow window centered around $q_{\mathbf{0}}^\star$ are transferred to e. Atoms with $q \neq q_{\mathbf{0}}^\star$ are off-resonant and remain in g. Next the detuning and Rabi frequency are quenched to the desired values $\Omega_{\mathbf{0}}$ and δ, and Rabi oscillations are recorded. Sequence II is identical, except that the initial pulse is about $-x$. Sequence III uses no initial pulse, but is otherwise the same as sequence I. The dynamics in I contains information about $\theta_{q_{\mathbf{0}}^\star}$, but this information will be buried in the signal of the $q \neq q_{\mathbf{0}}^\star$ atoms. Subtracting the dynamics of I and III isolates the dynamics of $q_{\mathbf{0}}^\star$ atoms. Sequence II is required because due to the mode dependence of $\Omega_{\mathbf{n}}$, a π-pulse is not experienced by all atoms populated at the transverse modes at high temperature. The dynamics of the atoms with $q_{\mathbf{0}}^\star$ that remain in g is cancelled by taking the average between sequences I and II, which effectively deals with only the atoms transferred to e. The dynamics for the sequences I, II, and III given in the main text are $S^z\left(\sqrt{1-f_{\mathbf{n}}^2}, -if_{\mathbf{n}}, t\right)$, $S^z\left(\sqrt{1-f_{\mathbf{n}}^2}, if_{\mathbf{n}}, t\right)$, and $S^z\left(1,0,t\right)$, respectively, where $f_{\mathbf{n}} \approx 1$ is the excitation fraction resulting from the initialization π-pulse. This gives the subtracted signal

$$\frac{S^z\left(\sqrt{1-f_{\mathbf{n}}^2}, -if_{\mathbf{n}}, t\right) + S^z\left(\sqrt{1-f_{\mathbf{n}}^2}, if_{\mathbf{n}}, t\right)}{2} - S^z\left(1,0,t\right) = f_{\mathbf{n}}^2\left(\cos^2\theta_{\mathbf{n}q} + \cos\left(2|B_{\mathbf{n}q}|t\right)\sin^2\theta_{\mathbf{n}q}\right). \tag{S31}$$

For a single frequency $|B_{\mathbf{n}q}|$, and $\theta_{\mathbf{n}q}$ can be inferred from these oscillations as $2\tan^2\theta_{\mathbf{n}q} = (\max - \min)/\text{mean}$. In the multiple-frequency case this is no longer a strict equality, but Fig. 2(b) shows that determining $\theta_{\mathbf{n}q}$ in this fashion from the thermal average of Eq. (S31) is nevertheless robust. In addition, the validity of this approach can be quantitatively estimated by the equality $(\max + \min)/\text{mean} = 2$, which employs the same assumptions.

Interacting dressed states with a sliding clock superlattice Here, we consider the dynamics of two atoms in neighboring sites $j_d(r)$ and $j_d(r)+1$ which are tunnel-coupled for a sliding lattice clock phase $\Delta\Upsilon = \pi$. We will take these two atoms to have different transverse mode indices $\mathbf{n}$ and $\mathbf{m}$. Interactions in the s-wave channel occur between these atoms when they are in an antisymmetric electronic state $|\Lambda_{\text{eg}}^-\rangle \equiv \left(|ge\rangle - |eg\rangle\right)/\sqrt{2}$ with a symmetric spatial wave function $|\Psi_{\mathbf{nm}}^+\rangle \equiv \left(|\mathbf{nm}\rangle_j + |\mathbf{mn}\rangle_j\right)$, with the subscript j denoting the lattice site index. Instead, p-wave interactions occur when the atoms are in a symmetric electronic state $|\Lambda_{\text{eg}}^+\rangle \equiv \left(|ge\rangle + |eg\rangle\right)/\sqrt{2}$ and an antisymmetric spatial wave function $|\Psi_{\mathbf{nm}}^-\rangle \equiv \left(|\mathbf{nm}\rangle_j - |\mathbf{mn}\rangle_j\right)$. For the purposes of describing the system dynamics at $\Delta\Upsilon = \pi$, where $|\rightarrow\rangle = \left(|g\rangle + |e\rangle\right)/\sqrt{2}$ is the single-well electronic ground state and $|\leftarrow\rangle = \left(|g\rangle - |e\rangle\right)/\sqrt{2}$ the excited state, it is useful to employ the states

$$\begin{aligned}
t,1 &: |2^{++},0\rangle, |0,2^{++}\rangle, |\rightarrow_{\mathbf{n}}, \rightarrow_{\mathbf{m}}\rangle, |\rightarrow_{\mathbf{m}}, \rightarrow_{\mathbf{n}}\rangle\,, \\
t,-1 &: |2^{--},0\rangle, |0,2^{--}\rangle, |\leftarrow_{\mathbf{n}}, \leftarrow_{\mathbf{m}}\rangle, |\leftarrow_{\mathbf{m}}, \leftarrow_{\mathbf{n}}\rangle \\
t,0 &: |2^{\pm},0\rangle, |0,2^{\pm}\rangle, \frac{|\rightarrow_{\mathbf{n}}, \leftarrow_{\mathbf{m}}\rangle - |\rightarrow_{\mathbf{m}}, \leftarrow_{\mathbf{n}}\rangle}{\sqrt{2}}, \frac{|\leftarrow_{\mathbf{n}}, \rightarrow_{\mathbf{m}}\rangle - |\leftarrow_{\mathbf{m}}, \rightarrow_{\mathbf{n}}\rangle}{\sqrt{2}} \\
s,0 &: |2^{\mp},0\rangle, |0,2^{\mp}\rangle, \frac{|\rightarrow_{\mathbf{n}}, \leftarrow_{\mathbf{m}}\rangle + |\rightarrow_{\mathbf{m}}, \leftarrow_{\mathbf{n}}\rangle}{\sqrt{2}}, \frac{|\leftarrow_{\mathbf{n}}, \rightarrow_{\mathbf{m}}\rangle + |\leftarrow_{\mathbf{m}}, \rightarrow_{\mathbf{n}}\rangle}{\sqrt{2}}\,,
\end{aligned} \tag{S32}$$

where

$$|2^{++}\rangle = |\rightarrow\rightarrow\rangle|\Psi_{\mathbf{nm}}^-\rangle\,, \tag{S33}$$

$$|2^{--}\rangle = |\leftarrow\leftarrow\rangle|\Psi_{\mathbf{nm}}^-\rangle\,, \tag{S34}$$

$$|2^{\pm}\rangle = \frac{|\rightarrow\leftarrow\rangle + |\leftarrow\rightarrow\rangle}{\sqrt{2}}|\Psi_{\mathbf{nm}}^-\rangle\,, \tag{S35}$$

$$|2^{\mp}\rangle = \frac{|\rightarrow\leftarrow\rangle - |\leftarrow\rightarrow\rangle}{\sqrt{2}}|\Psi_{\mathbf{nm}}^+\rangle\,. \tag{S36}$$

In each four-state sector the Hamiltonian may be written as

$$\hat{H}_{\mu,M_x} = 2M_x\Omega\mathbb{I} + \begin{pmatrix} U_{\mu,M_x} & 0 & J & J \\ 0 & U_{\mu,M_x} & -J & -J \\ J & -J & 0 & 0 \\ J & -J & 0 & 0 \end{pmatrix}, \tag{S37}$$

where $\mu = t, s$, $U_{t,M_x} = V_{M_x}$, $U_{s,0} = U_0$, $\mathbb{I}$ is the identity operator, and we have set $\Omega_{\mathbf{n}} = \Omega_{\mathbf{m}} = \Omega$ and $J_{\mathbf{n}} = J_{\mathbf{m}} = J$ for simplicity. The $s, 0$ singlet sector is rigorously decoupled from the others, but there is mixing between the triplet sectors proportional to the spin model parameters χ and C. These couplings are neglected due to the large single-particle energy difference $\sim \Omega$ between coupled manifolds with the assumed separation of energy scales $\Omega \gg J, V, U$.

The Hamiltonians Eq. (S37) may be readily diagonalized, leading to the eigenvalues $2M_x\Omega, 2M_x\Omega + U, 2M_x\Omega + \frac{U}{2} \pm \sqrt{4J^2 + \frac{U^2}{4}}$. At high temperatures compared to the tunneling, and for the adiabatic preparation procedure described in the main text, the observed dynamics will be an equal weight superposition of the dynamics from the initial states $|2^{++}, 0\rangle$, $|0, 2^{--}\rangle$, $|\rightarrow_{\mathbf{n}}, \leftarrow_{\mathbf{m}}\rangle$, and $|\rightarrow_{\mathbf{m}}, \leftarrow_{\mathbf{n}}\rangle$. The dynamics of the number of excitations following adiabatic conversion back to the "bare" g/e basis for these states are

$$|2^{++}, 0\rangle, |0, 2^{--}\rangle \to n_e(t) = 1 - \cos\frac{V_1 t}{2}\cos\left(t\sqrt{4J^2 + \frac{V_1^2}{4}}\right) - \frac{V_1 \sin\frac{V_1 t}{2}\sin\left(t\sqrt{4J^2 + V_1^2/4}\right)}{\sqrt{16J^2 + V_1^2}}, \tag{S38}$$

$$\begin{aligned} |\rightarrow_{\mathbf{n}}, \leftarrow_{\mathbf{m}}\rangle, |\rightarrow_{\mathbf{m}}, \leftarrow_{\mathbf{n}}\rangle \to n_e(t) =& 1 - \frac{1}{2}\left(\cos\frac{V_0 t}{2}\cos\left(t\sqrt{4J^2 + \frac{V_0^2}{4}}\right) + \cos\frac{U_0 t}{2}\cos\left(t\sqrt{4J^2 + \frac{U_0^2}{4}}\right)\right) \\ &- \frac{1}{2}\left(\frac{V_0 \sin\frac{V_0 t}{2}\sin\left(t\sqrt{4J^2 + V_0^2/4}\right)}{\sqrt{16J^2 + V_0^2}} + \frac{U_0 \sin\frac{U_0 t}{2}\sin\left(t\sqrt{4J^2 + U_0^2/4}\right)}{\sqrt{16J^2 + U_0^2}}\right). \end{aligned} \tag{S39}$$

For small interactions compared to tunneling, we can expand the result to lowest order in interactions, and find the thermally averaged dynamics

$$n_e(t) = 2\sin^2(Jt) - \frac{\left(U_0^2 + V_0^2 + 2V_1^2\right) t \left(\sin(2Jt) - 2Jt\cos(2Jt)\right)}{64J}. \tag{S40}$$

In addition to the above two-particle dynamics, there will be contributions from experimental realizations in which the resonant double well has only a single particle. Here, the dynamics is $n_e(t) = \sin^2(Jt)$. Writing p_1 as the probability of a single particle in a given double well and p_2 as the probability of having two particles, the small-interaction dynamics averaged over all realizations is hence

$$n_e(t) = (p_1 + 2p_2)\sin^2(Jt) - p_2\frac{\left(U_0^2 + V_0^2 + 2V_1^2\right) t \left(\sin(2Jt) - 2Jt\cos(2Jt)\right)}{64J}. \tag{S41}$$

Noting that $p_1 + 2p_2 = N$ is the average number, we can subtract the measurements of $n_e(t)/N$ for two different densities with single- and double-occupancy probabilities (p_1, p_2) and (p_1', p_2') and numbers N and N', respectively, to find

$$\Delta[n_e(t)/N] = -\left(\frac{p_2}{N} - \frac{p_2'}{N'}\right)\frac{\left(U_0^2 + V_0^2 + 2V_1^2\right) t \left(\sin(2Jt) - 2Jt\cos(2Jt)\right)}{64J}. \tag{S42}$$

In this way we separate the single-particle contrast decay due to a thermal spread in $J_{\mathbf{n}}$ from the contrast decay due to interactions.

Relative strength of ee losses for Sr. As shown in Ref. [1], at the mean-field level the time dependence of the coherence between the e and g states is affected by both elastic and inelastic processes. Here, we have in mind the Sr system, for which no eg losses have been measured [4]. While s-wave ee losses with associated scattering length $46a_0$ (a_0 the Bohr radius) have been measured for colliding particles with an antisymmetric nuclear spin state [4], these play no role for the nuclear-spin-polarized system we consider in this work. In the nuclear-spin-polarized case, only ee p-wave losses have a measurable effect, while elastic p-wave interactions occur in all (ee, eg, and gg) channels. The elastic processes are characterized by the quantity

$$B_{\text{eff}} = N\left(C - \chi\cos\theta\right), \tag{S43}$$

where C and χ were defined in Eqs. (S15)-(S16). Meanwhile, the inelastic processes are associated with the decay rate $\Gamma_{ee}N_e/2$. To estimate the relative effect of losses, we use that $\Gamma_{ee}/V^{ee} = \beta_{ee}^3/b_{ee}^3$, with b and β elastic and inelastic p-wave scattering parameters, measured to be $b_{eg}^3 = -169^3 a_0^3$, $b_{ee}^3 = -119^3 a_0^3$, $\beta_{ee}^3 = 125^3 a_0^3$, and $b_{gg}^3 = 74^3 a_0^3$ for Sr [4]. Using typical interrogation conditions of $\pi/2$ pulses in which $N_e = N/2$, we then find $|B_{\text{eff}}/(\Gamma_{ee}N_e/2)| = 2.14$, approximated as 2 in the main text.

[1] A. M. Rey, A.V. Gorshkov, C.V. Kraus, M. J. Martin, M. Bishof, M. D. Swallows, X. Zhang, C. Benko, J. Ye, N.D. Lemke, and A.D. Ludlow, Probing many-body interactions in an optical lattice clock, Annals Phys. 340, 311 - 351 (2014).

[2] Michael L. Wall, Kaden R. A. Hazzard, and Ana Maria Rey, Effective many-body parameters for atoms in nonseparable Gaussian optical potentials, Phys. Rev. A **92**, 013610 (2015).

[3] M. J. Martin, M. Bishof, M. D. Swallows, X. Zhang, C. Benko, J. von-Stecher, A. V. Gorshkov, A. M. Rey, and Jun Ye, A quantum many-body spin system in an optical lattice clock, Science **341**, 632 - 636 (2013).

[4] X. Zhang, M. Bishof, S. L. Bromley, C. V. Kraus, M. S. Safronova, P. Zoller, A. M. Rey, and J. Ye, Spectroscopic observation of SU(N)-symmetric interactions in Sr orbital magnetism, Science **345**, 1467 (2014).